JIPB Journal of Integrative Plant Biology

Breakthrough Report
https://doi.org/10.1111/jipb.13241

# Sphingolipid synthesis inhibitor fumonisin B1 causes verticillium wilt in cotton[FA]

Fan Xu†, Li Huang†, Junyao Wang, Caixia Ma, Yingqing Tan, Fanlong Wang, Yanhua Fan and Ming Luo*

Key Laboratory of Biotechnology and Crop Quality Improvement of the Ministry of Agriculture, Biotechnology Research Center, Southwest University, Chongqing 400716, China

†These authors contributed equally to this study.

*Correspondence: Ming Luo (luo0424@126.com)

Fan Xu

Ming Luo

## SUMMARY

Verticillium wilt caused by *Verticillium dahliae* is a major disease of cotton. Acidic protein–lipopolysaccharide complexes are thought to be the toxins responsible for its symptoms. Here, we determined that the sphingolipid biosynthesis inhibitor fumonisin B1 (FB1) acts as a toxin and phenocopies the symptoms induced by *V. dahliae*. Knocking out genes required for FB1 biosynthesis reduced *V. dahliae* pathogenicity. Moreover, we showed that overexpression of a FB1 and V. dahliae both downregulated gene, *GhIQD10*, enhanced verticillium wilt resistance by promoting the expression of brassinosteroid and anti-pathogen genes. Our results provide a new strategy for preventing verticillium wilt in cotton.

**Xu, F., Huang, L., Wang, J., Ma, C., Tan, Y., Wang, F., Fan, Y., and Luo, M.** (2022). Sphingolipid synthesis inhibitor fumonisin B1 causes verticillium wilt in cotton. J. Integr. Plant Biol. **64:** 836–842.

## INTRODUCTION

Cotton (*Gossypium hirsutum*) plants produce the most important natural textile fibers worldwide, accounting for approximately 35% of annual global fiber demands (Huang et al., 2021). Cotton yield losses are mainly due to verticillium wilt, the "cancer of cotton," a disease induced by the fungus *Verticillium dahliae* (*V. dahliae*) (Wang et al., 2020b). *Verticillium dahliae* is a soil-borne pathogen that causes vascular wilt in more than 200 dicotyledonous plant species, such as annual herbs, perennials, and woody plants (Li et al., 2020). The average yield loss of cotton caused by verticillium wilt is approximately 10%–35% (Li et al., 2019). The major mechanisms underlying wilt pathogenesis are xylem vessel blockage (Shaban et al., 2018) and toxin production (Luo et al., 2014). In the latter case, an acidic protein–lipopolysaccharide complex produced by *V. dahliae* functions as a toxin that seriously perturbs plant metabolism and carbon dioxide fixation and triggers degradation of $H_3PO_4$, eventually leading to plant death (Meyer et al., 1994; Luo et al., 2014).

*V. dahliae* necrosis- and ethylene-inducing protein (VdNEP) can induce necrotic lesions and trigger defense responses in *Nicotiana benthamiana*, *Arabidopsis thaliana*, and cotton plants (Wang et al., 2004; Zhou et al., 2012). Glycosylinositol phosphorylceramide (GIPC) sphingolipids act as receptors for this toxin (Lenarčič et al., 2017). In addition, the secondary metabolites of fungi are crucial players in fungal development and actively shape interactions with other organisms, especially those involved in pathogenesis (Keller, 2019). VdBre1 is required for cotton infection and contributes to pathogenicity by regulating lipid metabolism and secondary metabolism in *V. dahliae* (Wang et al., 2021a).

Here, we demonstrate that the sphingolipid biosynthesis inhibitor fumonisin B1 (FB1) is a metabolite produced in *V. dahliae* that likely functions as a virulence factor that contributes to verticillium wilt symptoms in cotton.

## RESULTS AND DISCUSSION

Treatment with FB1 caused a wilt and lesion mimic phenotype similar to the effects seen following *V. dahliae* treatment, but did not affect the vascular tissue of cotton plants. These symptoms were less serious than those induced by exposure to the toxin VdNLP1 or *V. dahliae* strain V991 (Figures 1A–C, S1).

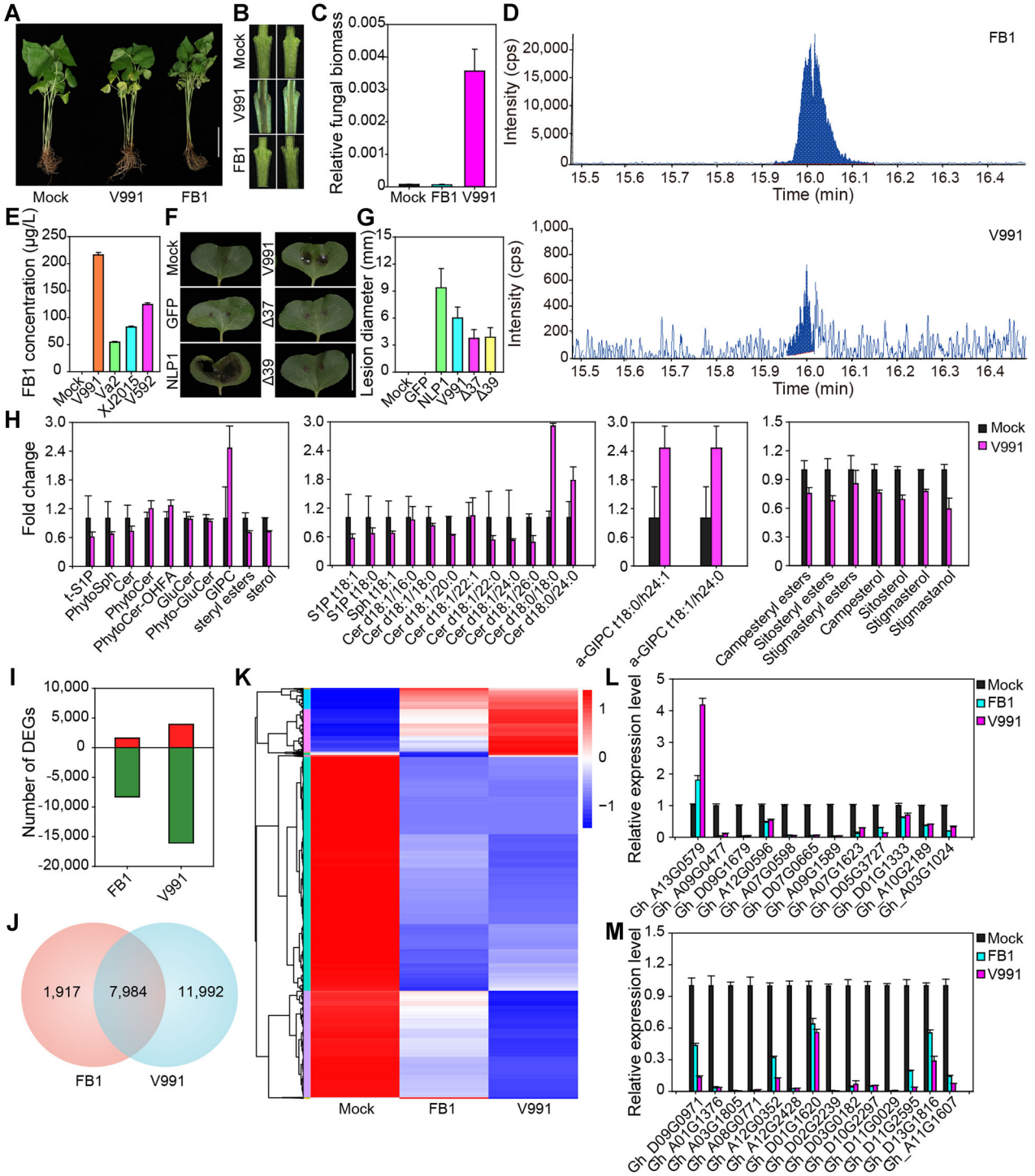


**Figure 1. Fumonisin B1 is one of the toxins in *Verticillium dahliae***

**(A–C)** Plant phenotypes **(A)**, stem longitudinal sections **(B)**, and *V. dahliae* biomass **(C)** in cotton seedlings at 7 d after treated with *V. dahliae* strain V991 and FB1. The cotton *GhHis* gene was used as the reference gene. **(D)** Mass spectrograms of standard FB1 (upper panel) and the aqueous metabolites of V991 (lower panel). **(E)** ELISA of FB1 in mock samples and *V. dahliae* strains V991, Va2, XJ2015, and V592. **(F and G)** The phenotypes **(F)** and lesion diameters **(G)** of cotton cotyledons at 7 d after treatment with the toxin protein VdNLP1, *V. dahliae* strain V991, and knockout strains Δ37 and Δ39. **(H)** Sphingolipid and sterol contents in cotton roots at 12 h after treatment with V991. tS1P, phytosphingosine-1-phosphate; PhytoSph, phytosphingosines; Cer, ceramides, PhytoCer, phytoceramides; PhytoCer-OHFA, phytoceramides with hydroxylated fatty acyls; GluCer, glucosylceramides; Phyto-GluCer, phyto-glucosylceramides; and GIPC, glycosyl inositol phosphorylceramide. **(I–K)** Statistical analysis of up- and down-regulated genes **(I)**, Venn diagram of differentially expressed genes (DEGs) **(J)**, and heat map of DEGs **(K)** in the transcriptomes of cotton roots at 12 h after treatment with V991 or FB1. **(L and M)** qRT-PCR of brassinosteroid- **(L)** and pathogenesis- **(M)** related genes in cotton roots treated with V991 or FB1. Error bars, ±SEM. Each analysis was repeated with three biological replicates.

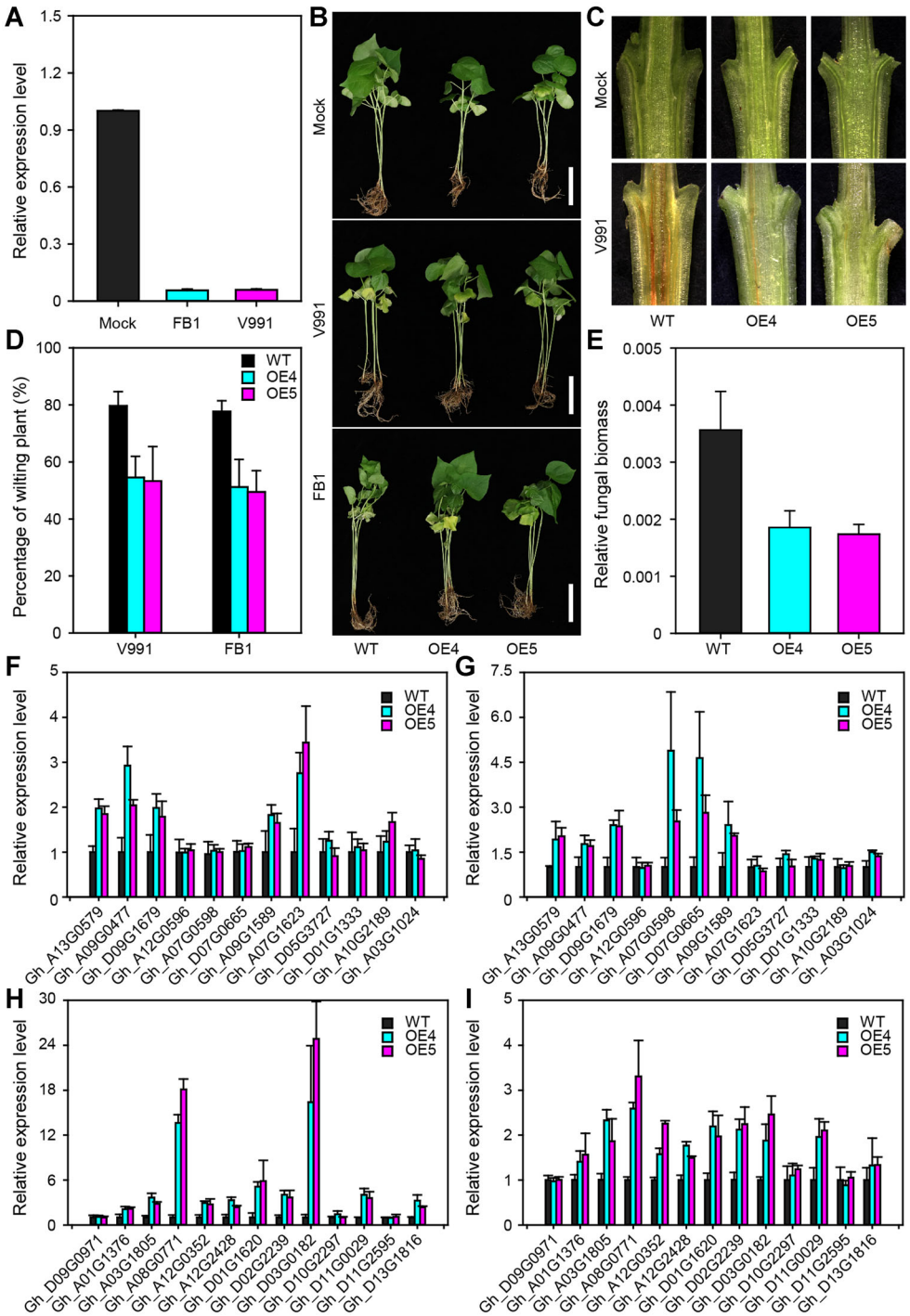


**Figure 2. *GhIQD10* promotes resistance to *Verticillium dahliae* in cotton**

**(A)** *GhIQD10* expression is suppressed by FB1 and *V. dahliae* treatment. **(B–E)** Phenotypes **(B)**, stem longitudinal sections **(C)**, wilting percentage **(D)**, and *V. dahliae* biomass **(E)** in the roots of *GhIQD10*-overexpression plants at 7 d after FB1 and *V. dahliae* treatment. **(F–I)** The expression of brassinosteroid- **(F and G)** and pathogenesis- **(H and I)** related genes in the roots of *GhIQD10*-overexpression plants at 7 d after treatment with FB1 **(F and H)** and *V. dahliae* **(G and I)**. Error bars, ±SEM. Each analysis was repeated with three biological replicates.

FB1 is a metabolite produced by *Fusarium moniliforme* that acts as an inhibitor of sphingolipid synthesis (Abbas et al., 1994). Blast search of the "antibiotics and secondary metabolite analysis shell (antiSMASH)" database (https://fungismash.secondarymetabolites.org/) (Blin et al., 2019), revealed a gene set that was identified as encoding a potential FB1 biosynthesis pathway in *V. dahliae* (Li et al., 2020) (Figure S1).

Ultra-high-performance liquid chromatography coupled to quadrupole Orbitrap high-resolution mass spectrometry (UHPLC-MS) performed on an aqueous extract of *V. dahliae* strain V991 as previously described (Tolosa et al., 2021) showed that the V991 strain synthesizes FB1 (Figure 1D). In addition, using an FB1 detection ELISA (enzyme-linked immunosorbent assay) kit (Shanghai Ruifan, China), we determined that the FB1 content was higher in *V. dahliae* strain V991 than in strains Va2, XJ2015, and V592 (Figure 1E). We then generated *V. dahliae* strains in which a genomic region including the gene set required for FB1 synthesis was knocked out (Figure S3) and found that this reduced the FB1 content (Figure S4) and the pathogenicity of each strain (Figure 1F, G). These results suggest that FB1, a metabolite of *V. dahliae*, might be a virulence factor that contributes to cotton wilt.

FB1 inhibits sphingolipid biosynthesis and therefore cotton fiber elongation by altering the sphingolipidome profile in cotton (Wang et al., 2020a). Using liquid chromatography tandem mass spectrometry (LC-MS/MS), we detected sphingolipids in cotton roots treated with *V. dahliae*. We found that those roots showed reduced levels of phytosphingosine-1-phosphate (t-S1P), phytosphingosines (PhytoSph), ceramides (Cer), glucosylceramides (GluCer), and phyto-glucosylceramides (Phyto-GluCer), but slightly elevated levels of phytoceramides (PhytoCer) and phytoceramides with hydroxylated fatty acyls (PhytoCer-OHFA); interestingly, the level of glycosyl inositol phosphorylceramide (GIPC) was significantly higher in *V. dahliae*-treated roots than in the untreated control roots.

We analyzed the sphingolipid molecules with markedly altered contents in more detail. Based on standard nomenclature, “d18:0” indicates that the long-chain bases of sphingolipids have two hydroxyl groups and 18 carbon atoms and no double bonds, and “t18:0” indicates that these bases have three hydroxyl groups and 18 carbon atoms and no double bonds. “18:0” indicates that the long-chain fatty acids of sphingolipids have 16–26 carbon atoms and no double bonds, and “h24:0” indicates that these groups are hydroxylated fatty acyls with 16–26 carbon atoms and no double bonds. The contents of both S1P t18:1 and S1P t18:0 for tS1P and Sph t18:1 for PhytoSph were strongly reduced in *V. dahliae*-treated roots versus the control. In *V. dahliae*-treated roots, the levels of ceramide molecules were slightly reduced, except for Cer d18:0/18:0 and Cer d18:0/18:0, whereas the levels of PhytoCer and PhytoCer-OHFA were noticeably higher (Figure 1H).

Intriguingly, the amounts of a-GIPC t18:0/h24:1 and a-GIPC t18:1/h24:0 in GIPC were significantly increased after infection with *V. dahliae* strain V991 (Figure 1H), but sharply reduced after FB1 treatment (Figure S5). Given that mutant plants with reduced GIPC contents are more resistant to NLP toxins than the wild type (Lenarčič et al., 2017), we suggest that FB1 produced by *V. dahliae* strain V991 disrupts sphingolipid biosynthesis in cotton and otherwise increases GIPC contents, making cotton more sensitive to its NLP toxins, and thereby causing cell death.

Sphingolipids play crucial roles in plant responses to biotic and abiotic stress (Luttgeharm et al., 2016). Jiang et al. showed that GIPC sphingolipids are important for the perception of salt by plants (2019). Phytosphingosines may regulate plasmodesma functions and cell-to-cell communication and maybe associated with resistance to plant pathogens (Liu et al., 2020). Sphingolipid-related components and genes might have pivotal roles in plant–pathogen interactions. In addition, sphingolipids and sterols are important components of membrane lipid rafts (Xu et al., 2020), and altered sphingolipid contents can affect the sterol content in plants (Valitova et al., 2016). The current results are consistent with these observations, as we also detected altered sterol compositions in *V. dahliae*-treated roots. Specifically, we observed a reduction in the abundance of both steryl esters and sterols (Figure 1H).

To further verify the relationship between *V. dahliae* and FB1, we analyzed the transcriptomes of cotton roots with or without FB1 or *V. dahliae* treatment using high-throughput RNA-Seq. We identified 1,608 upregulated and 8,293 downregulated differentially expressed genes (DEGs) following FB1, and 3,930 upregulated and 16,046 downregulated DEGs following *V. dahliae* treatment (Figures 1I, S6). Interestingly, most DEGs (80%) in FB1-treated roots were the same as those identified following *V. dahliae* treatment, and almost all of these DEGs showed similar expression trends after both treatments (Figure 1J, K).

Among the DEGs, genes related to the phytohormones auxin and cytokinin, which are closely related to plant growth (Kamiya, 2010), were downregulated following both treatments, indicating that both *V. dahliae* and FB1 inhibit plant growth (Figure S7). Brassinosteroids (BRs) function in plant–pathogen interactions and play important roles in shaping plant fitness and the growth–defense trade-offs (Nolan et al., 2020). We therefore surveyed the expression patterns of BR-related genes in the transcriptomic data. In agreement with previous findings, *GhBAK1* (Gh_A13G0579) was upregulated by both treatments, and other DEGs related to BR were suppressed by these treatments (Figure S8A). Furthermore, systemic acquired resistance typically involves the activation of pathogenesis-related (PR) genes (Burger and Chory, 2019). Indeed, PR-related DEGs were all repressed by both treatments (Figure S8B). Finally, our quantitative reverse-transcription PCR (qRT-PCR) results were consistent with the transcriptomic data (Figure 1L, M). These results indicate that the molecular responses to FB1 treatment were similar to those observed upon *V. dahliae* infection.

Extensive efforts have been made to breed cotton varieties resistant to verticillium wilt; cotton genes involved in this resistance are reviewed in Song et al. (2020). The tomato immune receptor Ve1 (Song et al., 2018), antifungal proteins (Wang et al., 2016; Wang et al., 2020b), and peptides (Tong et al., 2021) also play important roles in improving verticillium wilt resistance in cotton. Transcriptome analysis of FB1- and

*V. dahliae*-treated cotton roots revealed that IQ67-domain (IQD) protein-encoding genes were significantly downregulated following either FB1 or *V. dahliae* treatment (Figure S9). IQD proteins play critical roles in plant defense, organ development and shape, and drought tolerance (Guo et al., 2021).

The ectopic expression of *GhIQD14* led to the formation of twisted organs in *Arabidopsis* due to changes in secondary wall formation (Wang et al., 2021b), whereas knockdown of *GhIQD31* and *GhIQD32* downregulated the expression of stress-responsive genes, thereby increasing drought and salt stress sensitivity in cotton (Yang et al., 2019). We therefore generated *GhIQD10* (*Gh_D01G0420*) overexpression (Figure S10) and VIGS (virus-induced gene silencing; Figure S11) cotton plants and examined their performance following *V. dahliae* or FB1 treatment. The suppression of *GhIQD10* expression by FB1 and *V. dahliae* was confirmed by qRT-PCR (Figure 2A). *GhIQD10*-overexpression plants were significantly more resistant to FB1, V991, and VdNLP1 than the wild type (Figures 2B–E, S12A, B). By contrast, *GhIQD10*-VIGS plants were susceptibility to V991 (Figure S12C–F).

We observed changes in the expression of various BR-related genes in *GhIQD10*-overexpression plants after FB1 or *V. dahliae* strain V991 treatment, as follows: FB1 treatment significantly upregulated *Gh_A13G0579*, *Gh_A09G0477*, *Gh_D09G1679*, *Gh_A09G1589*, and *Gh_A07G1623*, and slightly increased the expression of *Gh_A10G2189*; V991 treatment clearly increased the expression of *Gh_A13G0579*, *Gh_A09-G0477*, *Gh_D09G1679*, *Gh_A07G0598*, *Gh_D07G0665*, and *Gh_A09G1589* and slightly upregulated *Gh_D05G3727*, *Gh_D01G1333*, and *Gh_A03G1024* (Figure 2F, G). The expression of almost all PR-related genes increased in the *GhIQD10*-overexpression lines after both treatments, but *Gh_A08G0771* and *Gh_D03G0182* were sharply upregulated upon FB1 treatment (Figure 2H, I). These results suggest that *GhIQD10* contributes to verticillium wilt resistance in cotton by activating BR signaling and PR-related gene expression regardless of whether the challenge is initiated by FB1 or V991.

Plant sphingolipids play a critical role in biotic stress responses by directing the cells to initiate programmed cell death (Ali et al., 2018). In the present study, we demonstrated that FB1, a sphingolipid biosynthesis inhibitor and metabolite of *V. dahliae*, acts as a pathogenic factor that causes wilt symptoms in cotton. Moreover, both FB1 and *V. dahliae* treatment downregulated *GhIQD10*, which confers verticillium wilt resistance in cotton in a BR- and PR-dependent manner. Sphingolipids are closely associated with cotton verticillium wilt tolerance in cotton. Our results provide new insights into the pathogenicity of *V. dahliae*, thereby revealing potential targets for breeding verticillium wilt-resistant cotton.

## ACKNOWLEDGEMENTS

We thank Professor Guo Huishan (Institute of Microbiology of the Chinese Academy of Sciences) for kindly providing the prokaryotic VdNLP1 expression vectors. This study was funded by the National Natural Science Foundation of China (31571722 and 31971984). We are grateful to Professor Ma Zhiying (Hebei Agricultural University) for kindly providing Jimian 14 seeds.

## CONFLICTS OF INTEREST

The authors declare that they have no conflicts of interest associated with this work.

## AUTHOR CONTRIBUTIONS

F.X. and M.L. designed experiments. F.X., L.H., C.M., J.W., Y. T., F.W., and Y.F. performed experiments. F.X. analyzed the data and drafted the manuscript. M.L. supervised the project. All authors have discussed the work and edited the manuscript.

**Edited by**: Suomeng Dong, Nanjing Agricultural University, China

**Received** Jan. 2, 2022; **Accepted** Mar. 1, 2022; **Published** Mar. 3, 2022

**FA:** Free Access

## REFERENCES

**Abbas, H.K., Tanaka, T., Duke, S.O., Porter, J.K., Wray, E.M., Hodges, L., Sessions, A.E., Wang, E., Merrill Jr., A.H., and Riley, R.T.** (1994). Fumonisin- and AAL-toxin-induced disruption of sphingolipid metabolism with accumulation of free sphingoid bases. Plant Physiol. **106:** 1085–1093.

**Ali, U., Li, H., Wang, X., and Guo, L.** (2018). Emerging roles of sphingolipid signaling in plant response to biotic and abiotic stresses. Mol. Plant **11:** 1328–1343.

**Blin, K., Shaw, S., Steinke, K., Villebro, R., Ziemert, N., Lee, S.Y., Medema, M.H., and Weber, T.** (2019). antiSMASH 5.0: Updates to the secondary metabolite genome mining pipeline. Nucleic Acids Res. **47:** W81–W87.

**Burger, M., and Chory, J.** (2019). Stressed out about hormones: How plants orchestrate immunity. Cell Host Microbe **26:** 163–172.

**Guo, C.Y., Zhou, J., and Li, D.W.** (2021). New insights into functions of IQ67-domain proteins. Front. Plant Sci. **11:** 614851.

**Huang, G., Huang, J.Q., Chen, X.Y., and Zhu, Y.X.** (2021). Recent advances and future perspectives in cotton research. Annu. Rev. Plant Biol. **72:** 437–462.

**Jiang, Z., Zhou, X., Tao, M., Yuan, F., Liu, L., Wu, F., Wu, X., Xiang, Y., Niu, Y., Liu, F., Li, C., Ye, R., Byeon, B., Xue, Y., Zhao, H., Wang, H. N., Crawford, B.M., Johnson, D.M., Hu, C., Pei, C., Zhou, W., Swift, G.B., Zhang, H., Vo-Dinh, T., Hu, Z., Siedow, J.N., and Pei, Z.M.** (2019). Plant cell-surface GIPC sphingolipids sense salt to trigger $Ca^{2+}$ influx. Nature **572:** 341–346.

**Kamiya, Y.** (2010). Plant Hormones: Versatile regulators of plant growth and development. Annu. Rev. Plant Biol. **61:** 1.

**Keller, N.P.** (2019). Fungal secondary metabolism: Regulation, function and drug discovery. Nat. Rev. Microbiol. **17:** 167–180.

**Lenarčič, T., Albert, I., Böhm, H., Hodnik, V., Pirc, K., Zavec, A.B., Podobnik, M., Pahovnik, D., Žagar, E., Pruitt, R., Greimel, P., Yamaji-Hasegawa, A., Kobayashi, T., Zienkiewicz, A., Gömann, J.,**

**Mortimer, J.C., Fang, L., Mamode-Cassim, A., Deleu, M., Lins, L., Oecking, C., Feussner, I., Mongrand, S., Anderluh, G., and Nürnberger, T.** (2017). Eudicot plant-specific sphingolipids determine host selectivity of microbial NLP cytolysins. Science **358:** 1431–1434.

**Li, H., Dai, J., Qin, J., Shang, W., Chen, J., Zhang, L., Dai, X., Klosterman, S.J., Xu, X., Subbarao, K.V., Fan, S., and Hu, X.** (2020). Genome sequences of *Verticillium dahliae* defoliating strain XJ592 and nondefoliating strain XJ511. Mol. Plant Microbe. Interact. **33:** 565–568.

**Li, Z.K., Chen, B., Li, X.X., Wang, J.P., Zhang, Y., Wang, X.F., Yan, Y.Y., Ke, H.F., Yang, J., Wu, J.H., Wang, G.N., Zhang, G.Y., Wu, L.Q., Wang, X.Y., and Ma, Z.Y.** (2019). A newly identified cluster of glutathione S-transferase genes provides verticillium wilt resistance in cotton. Plant J. **98:** 213–227.

**Liu, N.J., Zhang, T., Liu, Z.H., Chen, X., Guo, H.S., Ju, B.H., Zhang, Y.Y., Li, G.Z., Zhou, Q.H., Qin, Y.M., and Zhu, Y.X.** (2020). Phytosphinganine affects plasmodesmata permeability via facilitating PDLP5-stimulated callose accumulation in *Arabidopsis*. Mol. Plant **13:** 128–143.

**Luo, X.M., Xie, C.J., Dong, J.Y., Yang, X.Y., and Sui, A.P.** (2014). Interactions between *Verticillium dahliae* and its host: Vegetative growth, pathogenicity, plant immunity. Appl. Microbiol. Biot. **98:** 6921–6932.

**Luttgeharm, K.D., Kimberlin, A.N., and Cahoon, E.B.** (2016). Plant sphingolipid metabolism and function. Subcell. Biochem. **86:** 249–286.

**Meyer, R., Slater, V., and Dubery, I.A.** (1994). A phytotoxic protein-lipopolysaccharide complex produced by *Verticillium dahliae*. Phytochemistry **35:** 1449–1453.

**Nolan, T.M., Vukasinovic, N., Liu, D., Russinova, E., and Yin, Y.** (2020). Brassinosteroids: Multidimensional regulators of plant growth, development, and stress responses. Plant Cell **32:** 295–318.

**Shaban, M., Miao, Y.H., Ullah, A., Khan, A.Q., Menghwar, H., Khan, A. H., Ahmed, M.M., Tabassum, M.A., and Zhu, L.F.** (2018). Physiological and molecular mechanism of defense in cotton against *Verticillium dahliae*. Plant Physiol. Biochem **125:** 193–204.

**Song, R., Li, J., Xie, C., Jian, W., and Yang, X.** (2020). An overview of the molecular genetics of plant resistance to the verticillium wilt pathogen *Verticillium dahliae*. Int. J. Mol. Sci. **21:** 1120.

**Song, Y., Liu, L., Wang, Y., Valkenburg, D.J., Zhang, X., Zhu, L., and Thomma, B.** (2018). Transfer of tomato immune receptor Ve1 confers Ave1-dependent verticillium resistance in tobacco and cotton. Plant Biotechnol. J. **16:** 638–648.

**Tolosa, J., Rodriguez-Carrasco, Y., Graziani, G., Gaspari, A., Ferrer, E., Manes, J., and Ritieni, A.** (2021). Mycotoxin occurrence and risk assessment in gluten-free pasta through UHPLC-Q-exactive orbitrap MS. Toxins (Basel) **13:** 305.

**Tong, S., Yuan, M., Liu, Y., Li, X.B., Jin, D., Cheng, X., Lin, D.M., Ling, H. C., Yang, D.N., Wang, Y., Mao, A.J., Pei, Y., and Fan, Y.H.** (2021). Ergosterol-targeting fusion antifungal peptide significantly increases the verticillium wilt resistance of cotton. Plant Biotechnol. J. **19:** 926–936.

**Valitova, J.N., Sulkarnayeva, A.G., and Minibayeva, F.V.** (2016). Plant sterols: Diversity, biosynthesis, and physiological functions. Biochemistry (Mosc.) **81:** 819–834.

**Wang, H., Chen, B., Tian, J., and Kong, Z.** (2021a). *Verticillium dahliae* VdBre1 is required for cotton infection by modulating lipid metabolism and secondary metabolites. Environ. Microbiol. **23:** 1991–2003.

**Wang, J.Y., Cai, Y., Gou, J.Y., Mao, Y.B., Xu, Y.H., Jiang, W.H., and Chen, X.Y.** (2004). VdNEP, an elicitor from *Verticillium dahliae*, induces cotton plant wilting. Appl. Environ. Microbiol. **70:** 4989–4995.

**Wang, L., Liu, C., Liu, Y.J., and Luo, M.** (2020a). Fumonisin B1-induced changes in cotton fiber elongation revealed by sphingolipidomics and proteomics. Biomolecules **10:** 1258.

**Wang, L., Liu, Y.J., Liu, C., Ge, C.W., Xu, F., and Luo, M.** (2021b). Ectopic expression of *GhIQD14* (cotton IQ67 domain-containing protein 14) causes twisted organ and modulates secondary wall formation in *Arabidopsis*. Plant Physiol. Biochem. **163:** 276–284.

**Wang, Y., Liang, C., Wu, S., Jian, G., Zhang, X., Zhang, H., Tang, J., Li, J., Jiao, G., Li, F., and Chu, C.** (2020b). Vascular-specific expression of gastrodia antifungal protein gene significantly enhanced cotton verticillium wilt resistance. Plant Biotechnol. J. **18:** 1498–1500.

**Wang, Y., Liang, C., Wu, S., Zhang, X., Tang, J., Jian, G., Jiao, G., Li, F., and Chu, C.** (2016). Significant improvement of cotton verticillium wilt resistance by manipulating the expression of gastrodia antifungal proteins. Mol. Plant **9:** 1436–1439.

**Xu, F., Suo, X., Li, F., Bao, C., He, S., Huang, L., and Luo, M.** (2020). Membrane lipid raft organization during cotton fiber development. J. Cotton. Res. **3:** 9.

**Yang, X., Kirungu, J.N., Magwanga, R.O., Xu, Y.C., Pu, L., Zhou, Z.L., Hou, Y.Q., Cai, X.Y., Wang, K.B., and Liu, F.** (2019). Knockdown of *GhIQD31* and *GhIQD32* increases drought and salt stress sensitivity in *Gossypium hirsutum*. Plant Physiol. Biochem **144:** 166–177.

**Zhou, B.J., Jia, P.S., Gao, F., and Guo, H.S.** (2012). Molecular characterization and functional analysis of a necrosis- and ethylene-inducing, protein-encoding gene family from *Verticillium dahliae*. Mol. Plant Microbe. Interact. **25:** 964–975.

## SUPPORTING INFORMATION

Additional Supporting Information may be found online in the supporting information tab for this article: http://onlinelibrary.wiley.com/doi/10.1111/jipb.13241/suppinfo

**Figure S1**. The phenotypes of cotton cotyledon at 7 d after treatment with toxic protein VdNLP1

**(A)** The lesion phenotypes of cotton cotyledon at 7 d after treatment with toxic protein VdNLP1, *V. dahliae* strain V991, and FB1. **(B)** The lesion diameter of cotton cotyledon at 7 d after treatment with toxic protein VdNLP1, *V. dahliae* strain V991, and FB1. Error bars, ±SEM. Each analysis was repeated with three biological replicates.

**Figure S2**. BLAST analysis of the secondary metabolite cluster in *V. dahliae* genome

**(A)** The known secondary metabolite cluster in *V. dahliae* genome. yellow rectangle, known secondary metabolite cluster; indigo triangle, the known fumonisin B1 synthesis cluster. **(B)** The secondary metabolite cluster blasting results of *V. dahliae* genome on antiSMASH' database. **(C)** The annotation of indigo triangle indicated cluster in **(A)**.

**Figure S3**. Identification of *V. dahliae* knockout strain Δ37 and Δ39

**(A)** Schematic representation of the FB1 knockout vector. **(B–D)** The electrophoresis images of PCR identification for *V. dahliae* knockout *strain* Δ37 and Δ39 using the HygB **(B)**, Up **(C)**, and Down **(D)** primers as indicated in A.

**Figure S4**. FB1 contents in knockout *V. dahliae* strains

The ELISA detection of FB1 in *V. dahliae* strains V991, Δ37, and Δ39. Error bars, ±SEM. Each analysis was repeated with three biological replicates.

**Figure S5**. GIPC contents in FB1-treated cotton roots

GIPC contents in cotton roots at 12 h after treated with FB1. "t18:0" and "t18:1" indicate that the long-chain bases (LCB) of GIPC have three hydroxyl groups and 18 carbon atoms and no double bonds or one double bonds, respectively. "24:0" and "h24:1" indicate that the long-chain fatty acid (LCFA) of GIPC have 24 carbon atoms and no double bonds or are hydroxylated fatty acyl and have 24 carbon atoms and one double bond, respectively. Error bars, ±SEM. Each analysis was repeated with three biological replicates.

**Figure S6**. Volcano plot of DEGs in FB1- and V991-treated cotton roots

**(A and B)** The volcano plot up- and down-regulated differentially expressed genes (DEGs) in cotton roots at 12 h after treated with FB1 **(A)** and *V. dahliae* strain V991 **(B)**. Red rhombus, up-regulated DEGs. Green square, down-regulated DEGs. Gray dot, undifferentiated expression genes.

**Figure S7**. The expression of cytokinin- and auxin-related genes in FB1- and V991-treated cotton roots

**(A and B)** The expression heat map of Cytokinin- **(A)** and Auxin- **(B)** related genes in cotton roots at 12 h after treated with FB1 and *V. dahliae* strain V991. The color scale indicates the LOG2 (transcript abundance of FB1 or V991 treatment/the mock): red, increase in transcript abundance; blue, decrease in transcript abundance. Gene_id, the

accession number of related genes. Gene description, the annotation of related genes.

**Figure S8**. The expression of brassinosteroid- and pathogenesis-related genes in FB1- and V991-treated cotton roots

**(A and B)** The expression heat map of brassinosteroid - **(A)** and pathogenesis- **(B)** related genes in cotton roots at 12 h after treated with FB1 and *V. dahliae* strain V991. The color scale indicates the LOG2 (transcript abundance of FB1 or V991 treatment/the mock): red, increase in transcript abundance; blue, decrease in transcript abundance. Gene_id, the accession number of related genes. Gene description, the annotation of related genes.

**Figure S9**. The expression of IQ67-domain (IQD) family genes in FB1- and V991-treated cotton roots

The expression of heat map of IIQD family genes in cotton roots at 12 h after treated with FB1 and *V. dahliae* strain V991. Indigo triangle, *GhIQD10*. The color scale indicates the LOG 2 (transcript abundance of FB1 or V991 treatment/the mock): red, increase in transcript abundance; blue, decrease in transcript abundance. Gene_id, the accession number of related genes. Gene description, the annotation of related genes. Bright blue triangle, A and D sub-genome *GhIQD10*.

**Figure S10**. Identification of *GhIQD10*-overexpression cottons

**(A)** Schematic representation of the *GhIQD10* overexpression vector. LB and RB, T-DNA left and right border. 35S, CaMV35S promoter. Ter, terminator. GUS-NPTII, fusion gene of GUS and NPTII. 35S96F and IQD10OER, primers for transgenic cotton identification. **(B)** The electrophoresis images of PCR identification for *GhIQD10*-overexpression cottons using primer indicated in A. M, Marker; + positive plasmids; -, negative control; WT, wild type; OE4 and OE5, overexpression lines. **(C)** The expression of *GhIQD10* in its overexpression lines. Error bars, ±SEM. Each analysis was repeated with three biological replicates.

**Figure S11**. Identification of *Gh_IQD10* VIGS (virus induced gene silencing) cotton lines

**(A)** Phenotypes of *Gh_IQD10* VIGS cotton. VIGS (+), VIGS positive lines (albino). VIGS (-), VIGS negative lines. V1 and V2, *Gh_IQD10* VIGS lines. **(B)** The expression of *GhIQD10* in its VIGS lines. Error bars, ±SEM. Each analysis was repeated with three biological replicates.

**Figure S12**. Phenotypes of *Gh_IQD10* VIGS lines after *V. dahliae* V991 treatment

**(A and B)** The lesion phenotypes and diameters of *Gh_IQD10* overexpression cotton cotyledons at 7 d after treatment with the toxin protein VdNLP1 and *V. dahliae* strain V991. **(C–F)** Phenotypes **(C)**, stem longitudinal sections **(D)**, wilting percentage **(E)**, and *V. dahliae* biomass **(F)** of *GhIQD10* VIGS line roots at 7 d after treated with FB1 and *V. dahliae*. Error bars, ±SEM. Each analysis was repeated with three biological replicates.

**Table S1**. List of primers used for qRT-PCR

**Table S2**. List of primers used for vector construction

**Table S3**. Brassinosteroid-related gene expression levels and annotation

**Table S4**. Pathogenesis-related gene expression levels and annotation